

ORIGINAL PAPER

Comparative Ultrastructure of Fornicate Excavates, Including a Novel Free-living Relative of Diplomonads: *Aduncisulcus paluster* gen. et sp. nov.



Naoji Yubuki^{1,2}, Sam S.C. Huang, and Brian S. Leander

The Departments of Botany and Zoology, Beaty Biodiversity Research Centre and Museum, University of British Columbia, Vancouver, British Columbia, V6T 1Z4, Canada

Submitted March 30, 2016; Accepted October 10, 2016
Monitoring Editor: Barry S. C. Leadbeater

The Fornicata (Excavata) is a group of microbial eukaryotes consisting of both free-living lineages (e.g., *Carpediemonas*) and parasitic lineages (e.g. *Giardia* and *Retortamonas*) that share several molecular and ultrastructural traits. *Carpediemonas*-like organisms (CLOs) are free-living lineages that diverged early within the Fornicata, making them important for inferring the early evolutionary history of the group. Molecular phylogenetic analyses of free-living fornicates, including sequences from environmental PCR surveys, have demonstrated that CLOs form six different lineages. Representatives from five of these lineages have been studied at the ultrastructural level. The sixth lineage has been labeled “CL2” but has yet to be described with ultrastructural data. Improved understanding of CL2 is expected to help elucidate character evolution within the Fornicata. Therefore, we comprehensively characterized CL2 (NY0171) in order to understand the ultrastructural traits in this lineage, especially the organization of the microtubular root system (i.e., the flagellar apparatus). CL2 shared several morphological features with other fornicates, including reduced mitochondria and an arched B fiber bridging flagellar roots 1 and 2. The molecular phylogenetic position combined with some distinctive ultrastructural traits (e.g., a curved ventral groove) in CL2 required us to establish a new genus and species, *Aduncisulcus paluster* gen. et sp. nov.

© 2016 Elsevier GmbH. All rights reserved.

Key words: Culturing; cytoskeleton; evolution; flagellar apparatus; morphology; ultrastructure.

Introduction

Comparative ultrastructural data from unicellular eukaryotes (protists) within a molecular phyloge-

netic context has provided important insights into the diversity and evolution of eukaryotic cells. Traits associated with the microtubular root systems of protists (i.e., the flagellar apparatus) are particularly informative because they can be compared across the tree of eukaryotes and demonstrate broad patterns of morphological evolution within each major clade (Moestrup 2000; Yubuki and Leander 2013; Yubuki et al. 2016). The unity and diversity of the

¹Corresponding author; fax +420 221 95 1841

²Present address: Departments of Parasitology and Zoology, Faculty of Science, Charles University, Vinicna 7, Prague, 128 44, Czech Republic
e-mail yubukin@natur.cuni.cz (N. Yubuki).

flagellar apparatus suggests that this cytoskeletal system was already complex in the most recent ancestor of all eukaryotes and was similar to those found in modern day excavates (Yubuki and Leander 2013). The Excavata is one of five eukaryotic supergroups, along with the Opisthokonta (Animalia, Fungi and their relatives), Amoebozoa, Archaeplastida and SAR (Stramenopile, Alveolata, Rhizaria) (Adl et al. 2012; Simpson 2003; Simpson and Roger 2004; Simpson et al. 2006). The Excavata includes single-celled organisms with different modes of nutrition, such as phototrophic microalgae (e.g., *Euglena*), human parasites (e.g., *Giardia* and *Naegleria*), free-living phagotrophic flagellates (e.g., *Carpodiemonas*) and intestinal symbionts (e.g., *Trichonympha* and *Monocercomonoides*).

The diversity within the excavate lineage Fornicata has played a prominent role in reconstructing the earliest stages of eukaryote evolution. The traits associated with the Fornicata are particularly important for inferring the evolutionary transition(s) from free-living modes of life to parasitic/commensal modes of life. Fornicates are flagellates that inhabit low oxygen environments, such as aquatic sediments and the intestines of animals. All members of this group lack conventional mitochondria and instead have modified/reduced forms (e.g., hydrogenosomes and mitosomes) referred to as “mitochondrion-related organelles” (MROs) (Cavalier-Smith 1998; Simpson 2003; Stairs et al. 2015; Takishita et al. 2012). The Fornicata include several different free-living lineages, called “*Carpodiemonas*-like organisms” (CLOs) (Kolisko et al. 2010), and mostly parasitic and commensal lineages within the Retortamonadida (*Retortamonas* and *Chilomastix*) and Diplomonadida (e.g., *Giardia*); however, there are also a few examples of free-living species within retortamonads and diplomonads, such as *Chilomastix cuspidata* and *Trepomonas agilis* (Silberman et al. 2002; Brugerolle and Lee 2000). Until recently, *Carpodiemonas membranifera* was the only representative of free-living fornicates (Simpson and Patterson 1999; Simpson et al. 2006). Over the last decade, five additional CLO clades have been identified: *Dysnectes* (Yubuki et al. 2007), *Hicanonectes* (Park et al. 2009), *Ergobibamus c* (Park et al. 2010), *Kipferlia* (Kolisko et al. 2010; Yubuki et al. 2013) and an undescribed lineage called “CL2” (Kolisko et al. 2010; Takishita et al. 2012). The ultrastructure of the flagellar apparatus in CLOs, excluding CL2, has been characterized previously and encompasses a great deal of variability in traits that reflect phylogenetic relationships. Molecular phylogenetic analyses of small subunit (SSU) rDNA

and six different protein gene sequences demonstrated that CLOs are distributed throughout the Fornicata within several different subclades: (i) *Dysnectes*, *Kipferlia*, retortamonads and diplomonads; (ii) *Hicanonectes*, *Ergobibamus* and CL2; and (iii) *Carpodiemonas* (Takishita et al. 2012).

In order to understand the unity and diversity within the Fornicata more comprehensively, we characterized the ultrastructure of CL2 using the same strain (NY0171) included in previous molecular phylogenetic analyses (Kolisko et al. 2010; Takishita et al. 2012). Prior to this study, the morphology of CL2 was known only from two light micrographs. Our investigation of the ultrastructural traits in CL2 combined with its molecular phylogenetic position enabled us to establish a new genus and species, *Aduncisulcus paluster* gen. et sp. nov.

Results

The General Morphology of *Aduncisulcus paluster* gen. et sp. nov. (NY0171)

The cells were 8.9 μm (7.0–11.3 μm , $n = 30$) long, 5.4 μm (4.1–7.2 μm , $n = 30$) wide and had a broad ventral groove that extended from just below the anterior end of the cell and curved toward the left over the posterior end of the cell (Figs 1, 2). The cells had two flagella inserted at the anterior end of the cell (Figs 1, 2). Flagellum 1 (F1) extended posteriorly within the ventral groove, was twice the length of the cell, and moved with rapid sinusoidal waves (Fig. 1A–C). F1 was adorned with a long ventral vane and a diminutive dorsal vane (Figs 2, 3A–C). The ventral vane was supported by a densely striated fibrous lamellum (Fig. 3A–D) and terminated at the posterior end of the ventral groove (Fig. 2). The anterior flagellum 2 (F2) did not possess vanes, extended laterally to the left side of the cell and moved rhythmically from anterior to posterior (Figs 1A, B, 2, 4A). The cells often attached to substrates using the tip of the posterior F1 (Fig. 1D). When the culture was disturbed, the cells swam slowly in a spiral pattern. Food particles were drawn into the ventral groove in currents generated by F1 and subsequently ingested by a cytostome positioned at the posterior end of the groove.

The nucleus was situated immediately behind the flagellar apparatus (Fig. 3A, B). The cells contained several mitochondrion-related organelles (MROs) that lacked cristae and were enveloped by two membranes (Fig. 4B). These organelles were ca. 400 nm long and were positioned mostly within the anterior half of the cell (Figs 5, 6). The ER

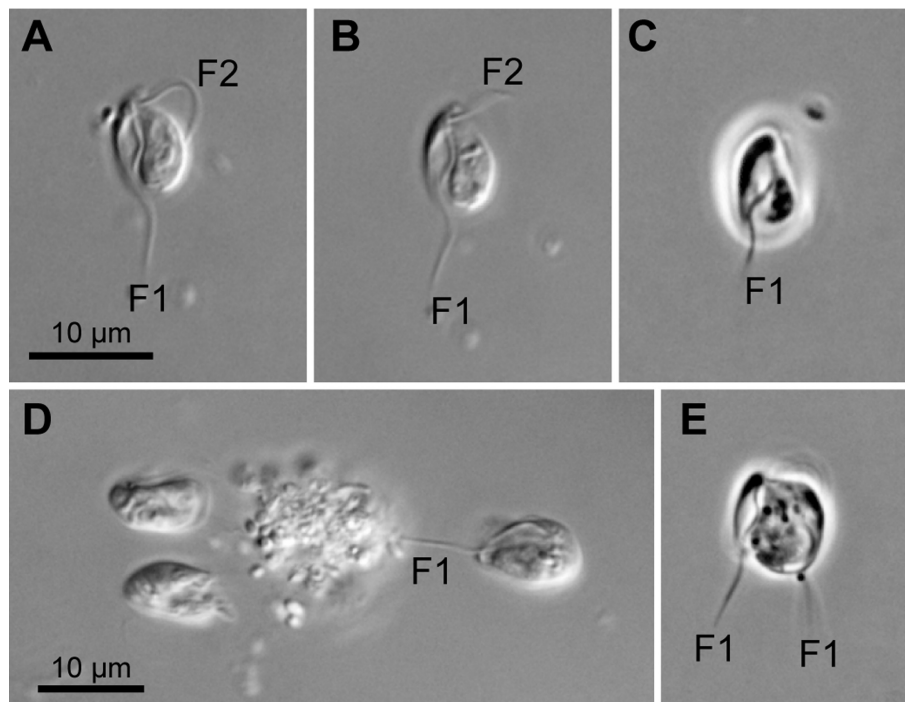


Figure 1. Light micrographs of living cells of *Aduncisulcus paluster* gen. et sp. nov. (NY0171). F1 = flagellum 1; F2 = flagellum 2. **A-B.** Differential interference contrast images showing general features of the cell. **C.** Phase contrast image. **D.** Three cells attached to a bacterial aggregate using the tips of the posterior flagella, F1. **E.** Phase contrast image of dividing cell. The scale bars in **A** and **D** are applicable for **B-C** and **E**, respectively.

enveloped the periphery of the cell just beneath the plasma membrane but was absent within the ventral groove (Fig. 3A, B). The cells reproduced by asexual division (Figs 1E, 4C). Dividing cells with two F1s, two F2s and two ventral grooves were observed under LM and TEM (Figs 1E, 4C). The flagellar apparatus was fully formed prior to cytokinesis (Fig. 4C).

Organization of the Flagellar Apparatus

The overall organization of the flagellar apparatus in *A. paluster* was similar to other CLOs studied previously (Park et al. 2009, 2010; Simpson and Patterson 1999; Yubuki et al. 2007, 2013). We applied the same terminology for the microtubular roots, basal bodies and flagella as used for the CLO *Kipferlia bialata* (Yubuki et al. 2013), which corresponds to the universal terminology for the flagellar apparatus in eukaryotes as a whole (Moestrup 2000; Yubuki and Leander 2013). Root 1 (R1), root 2 (R2) and root 3 (R3) in *K. bialata* and *A. paluster* correspond to the left root (LR), right root (RR) and anterior root (AR) in *D. brevis*, *H. teleskopos* and *E. cyprinoides*. Four basal bodies were present in most interphase cells of *A. paluster*. Only two basal bodies were found in a few cells, which

presumably represent newly formed daughter cells. Two basal bodies, B1 and B2, were associated with F1 and F2, respectively. B1 extended posteriorly and was situated at a right angle to B2 (Fig. 4A). An extra basal body was located on the left side of B1 and behind R1 (Fig. 5 B-C); another extra basal body was situated near the right side of B1 (Fig. 5 H). Three microtubular roots, namely root 1 (R1), root 2 (R2) and the singlet root (SR) and four fibrous structures, namely the A fiber, B fiber, C fiber and I fiber, were associated with B1. Only one microtubular root, namely root 3 (R3), was associated with B2.

Root 1 and associated B and C fibers. R1 originated from the ventral left side of B1 and extended posteriorly. The number of microtubules in R1 increased incrementally one at a time as the root extended from B1 to the left side of the cell, eventually reaching a total of eight (Figs 5A-G, 6). As R1 extended posteriorly, at least two inner (right) microtubules became disassociated with the rest (Figs 5G, 6C-F). The main portion of R1 supported the left edge of the ventral groove (Figs 5G, 6D-F). Two fibrous structures, namely the B fiber and C fiber, were associated with R1. The thin C fiber was associated with the dorsal side of R1 at the proxi-

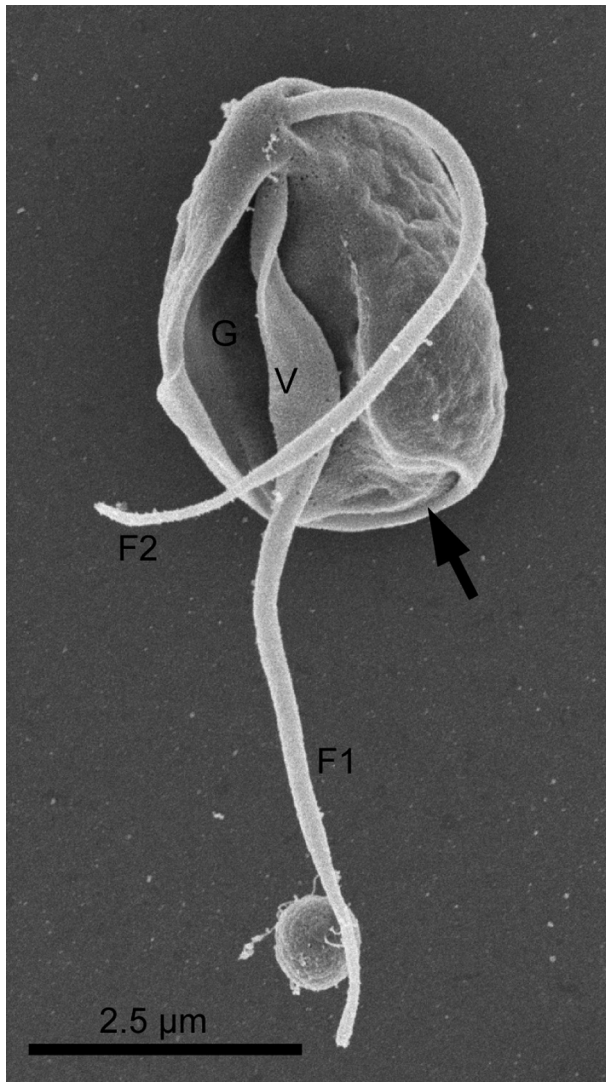


Figure 2. Scanning electron micrograph of *Aduncisulcus paluster* gen. et sp. nov. (NY0171) showing features on the ventral side of the cell. F1 = flagellum 1; F2 = flagellum 2; G = groove; V = ventral vane. Arrow indicates cytostome.

mal end (Fig. 5H, I). The thick B fiber attached to the right side of the R1 and stretched to the right side of the cell along the ventral side of B1 until it connected to the right side of R2. The B fiber extended posteriorly and supported the right side of the ventral groove (Fig. 5A-F).

Root 2, the singlet root and associated A and I fiber. R2 originated from the right dorsal side of B1, consisted of nine microtubules at its origin, and formed a concave face toward the ventral side of the cell. As R2 extended posteriorly, the number of microtubules increased to 16 near the inser-

tion of F1 (Fig. 7A-D). R2 split into two subunits: six microtubules formed an inner R2 (iR2) and 10 microtubules formed an outer R2 (oR2) (Fig. 7E). The iR2 extended toward the posterior end of the cell and supported the deepest region of the ventral groove (Fig. 7E, F). As oR2 extended posteriorly to support the right side of the ventral groove, the number of microtubules present increased to at least 38 (Figs 6, 7G). The iR2 was positioned between the nucleus and the cell membrane over the ventral groove (Figs 6, 7B-F).

The singlet root (SR) consisted of only one microtubule that originated from the dorsal side of B1 within the A fiber (Figs 5B, 7B). The SR extended posteriorly under the cell membrane and was situated between R1 and R2 along the entire length of the cell (Figs 5B-G, 7B-G). Like R2, the SR was squeezed between the nucleus and the plasma membrane. The A fiber connected the dorsal side of R2 to the dorsal sides of B1 and R1 (Figs 5A-F, H, 6A, B). The I fiber was a crosshatched structure that attached to the ventral (concave) side of R2 before it split into the iR2 and oR2 (Fig. 7A-D); the I fiber was restricted to oR2 after the splitting of R2 (Fig. 7E-G). The I fiber fused with the B fiber near the middle of the cell (Fig. 7F, G). Both the iR2 and oR2 curved inward near the posterior end of the cell to support the feeding apparatus (Fig. 8). The cytopharynx was situated between these two roots (Fig. 8).

Root 3 and associated structures. R3 originated from the proximal end of B2 and extended to the left side of the cell; R3 was oriented at about 45 degrees to the axis of B2 (Fig. 9A). At its origin, R3 consisted of one microtubule, but the number of microtubules increased up to five at the distal region of this root (Fig. 9). R3 was at least 1 μm long. An electron dense fiber connected B2 to with the dorsal side of R3 (Fig. 9B-E). A dorsal fan (F) of cytoskeletal microtubules ran in parallel to R3 just beneath the cell membrane (Fig. 9); the dorsal fan originated near the distal region of R3 and extended posteriorly along the cell surface until it became almost parallel with oR2 (Figs 9g, 10).

Discussion

The molecular phylogenetic position of *A. paluster* (as NY0171) was established previously to fall within the Fornicata, more precisely within the CLO clade consisting of *Hicanonectes* and *Ergobibamus* (Takishita et al. 2012) (Fig. 10). The ultrastructural traits of *A. paluster* described here, specifically the ventral feeding groove, flagellar vanes on the pos-

Table 1. Morphological characters of *Adaucisulcus paluster* gen. nov. et sp. nov. compared with other member of CLOs.

Taxon	Cell shape	Habitat	Ventral groove	Discrete Cytopharynx	Basal Bodies (#)	Flagella (#)	Flagellar vane (#)	R1	R2	B fiber down R1	Dorsal fan
<i>Dysnectes brevis</i>	Bean-shaped	Marine	+	–	2	2	2	+	+	+	–
<i>Iotanema spirale</i>	Spiral	Endobiotic	–	–	4	1	–	+	–	–	+
<i>Carpediemonas membranifera</i>	Bean-shaped	Marine	+	–	3	2	3	+	+	–	+
<i>Kipferlia bialata</i>	Bean-shaped	Marine	+	+	4	2	1	+	+	+	–
<i>Hicanonectes teleskopos</i>	Ovoid	Marine	+	+	4	2	2	+	+	–	+
<i>Ergobibamus cyprinoides</i>	Bean-shaped	Marine	+	–	4	2	2	+	+	+	+
<i>Adaucisulcus paluster</i>	Bean-shaped	Marine	+	+	4	2	2	+	+	–	+

+, present; –, absent.

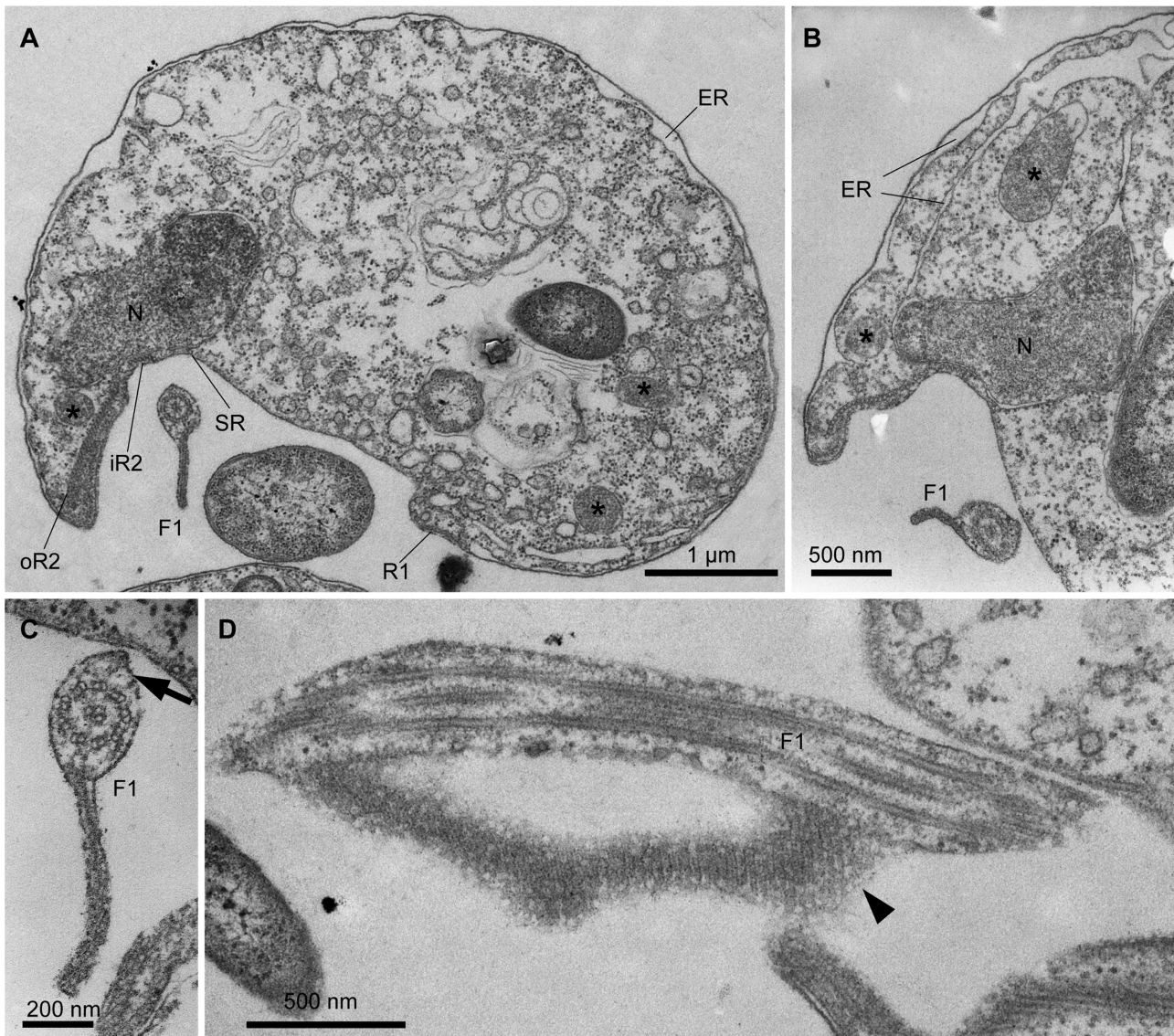


Figure 3. Transmission electron micrographs of *Aduncisulcus paluster* gen. et sp. nov. (NY0171) showing the general ultrastructure of the cell. F1 = flagellum 1; F2 = flagellum 2; iR2 = inner root 2; N = nucleus; oR2 = outer root 2; SR = singlet root. Arrow, arrowhead and asterisk indicate dorsal vane on F1, striated fibrous structure on F1 and a mitochondrion-related organelle (MRO), respectively. **A.** Transverse section of the cell demonstrating the ER lying below the peripheral area of the cell, except within the ventral groove. **B.** Transverse section showing the ER network developing from the nuclear envelope. **C.** Transverse section of F1 showing the long ventral vane and a small dorsal vane. **D.** Sagittal section of F1 showing the striations in the ventral vane.

terior flagellum and four microtubular roots (R1, R2, R3 and SR), reinforce the molecular phylogenetic data (Simpson and Roger 2004; Simpson 2003). *Aduncisulcus paluster* shared several traits with most other CLOs, such as being a small (< 13 µm) biflagellate living in a low oxygen marine habitat, having an arched B fiber between R1 and R2 and having MROs (Table 1; Fig. 10, position 2) (See Kolisko et al. 2010 for an exception to this typi-

cal combination of traits such as an uniflagellate, PCS isolate). However, each species of CLO differs in their cell size, cell shape, length of flagella, swimming behavior, details of the flagellar apparatus and molecular phylogenetic position (Kolisko et al. 2010; Takishita et al. 2012). *Aduncisulcus paluster* can be distinguished from all other CLOs under the light microscope by observing the curved ventral groove and the way the tip of the poste-

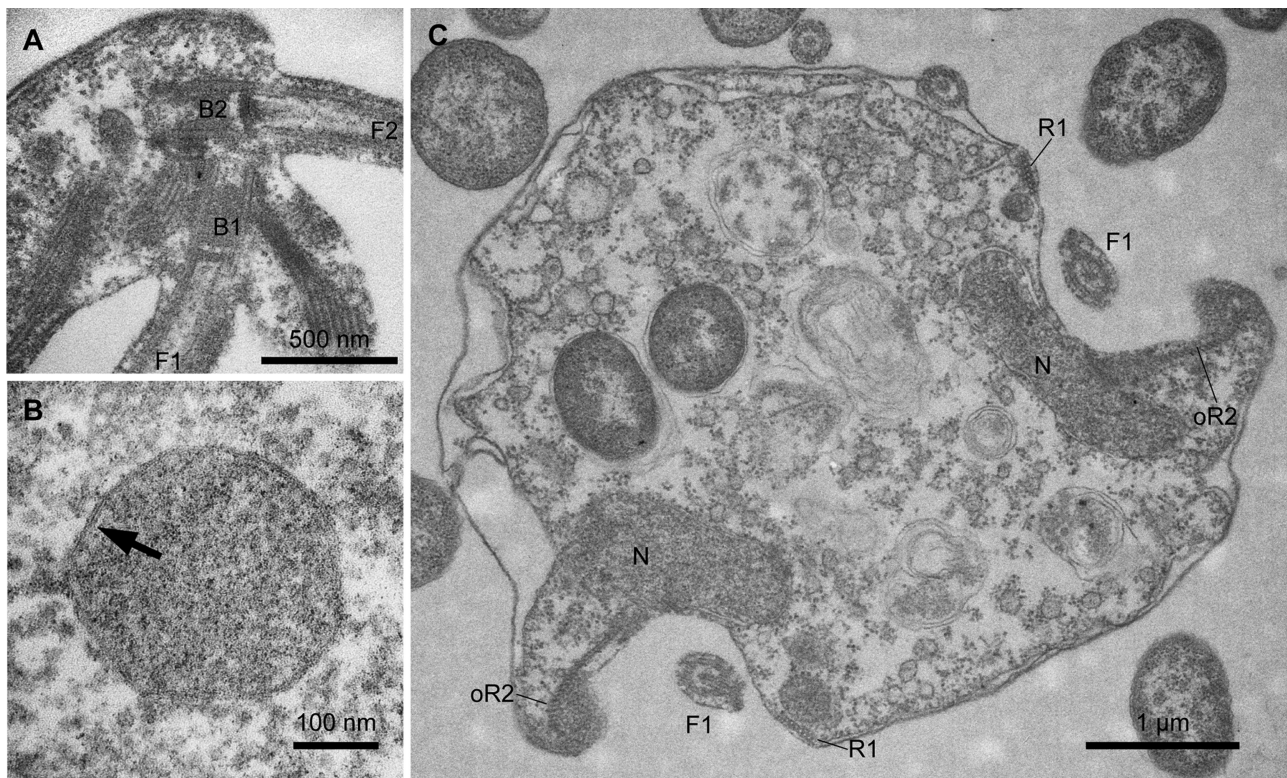


Figure 4. Transmission electron micrographs of *Aduncisulcus paluster* gen. et sp. nov. (NY0171) showing the general ultrastructure of the cell. **A.** Section through the anterior region of the cell showing the orientation of the two basal bodies. **B.** High magnification view of a mitochondrion-related organelle (MRO) with two enveloping membranes (arrow). **C.** Transverse section through a dividing cell.

rior F1 attaches to the substrate (Fig. 11, position 5). *Dysnectes brevis* also attaches to substrates with the posterior part of the cell, but not with F1 (Yubuki et al. 2007). Likewise, the retortamonad *Chilomastix* attaches to substrates using a distinctive posterior cell projection, called a “posterior spike”, but not with F1 (Bernard et al. 1997).

The molecular phylogenetic data (Fig. 11) suggests that the ultrastructure of *A. paluster* should be most similar to *Hicanonectes teleskopos*; both of these species share a curved ventral groove, which reflects a conspicuous cytopharynx (Park et al. 2009) (Fig. 11, position 4). *Hicanonectes teleskopos* has an oval cell shape and posterior F1 is 2.5–3.5 times longer than the length of the cell; *A. paluster*, by contrast, has a bean-shaped cell and relatively short flagella (Figs 1, 2). *Aduncisulcus paluster* and *H. teleskopos* share a reduced (thin) C fiber on R1, which differs from the multi-layered (thicker) structures found in other CLOs and excavates as a whole (Fig. 11, position 4). *Aduncisulcus paluster* and *H. teleskopos* shared a conspicuous cytopharynx. However, the cytopharynx in other CLOs, such as *Kipferlia bialata*, is

difficult to observe under light microscopy and requires the use of scanning electron microscopy (Yubuki et al. 2013). Nonetheless, a conspicuous cytopharynx has also been observed in *Chilomastix* (Bernard et al. 1997), *Retortamonas* (Brugerolle 1977) and *Trimastix* (O’Kelly et al. 1999; Simpson et al. 2000), suggesting that this trait was inherited from the most recent ancestor of metamonads (Fig. 11, position 1). The anterior R3 in *A. paluster*, *H. teleskopos* and *Ergobibamus cyprinoides* is more robust than in other CLOs, consisting of five, nine and six microtubules, respectively; R3 in other CLOs consists of only one or two microtubules. The robust R3, consisting of at least 6 microtubules, is inferred to be a derived state for the clade consisting of *Aduncisulcus*, *Hicanonectes* and *Ergobibamus* (Fig. 11, position 3).

Improved understanding of CLO diversity is beginning to shed considerable light onto the earliest stages in the evolution of fornicates and excavates as a whole. For instance, a detailed ultrastructural investigation of *K. bialata* provided important information about the excavate flagellar apparatus and its transformation during cell

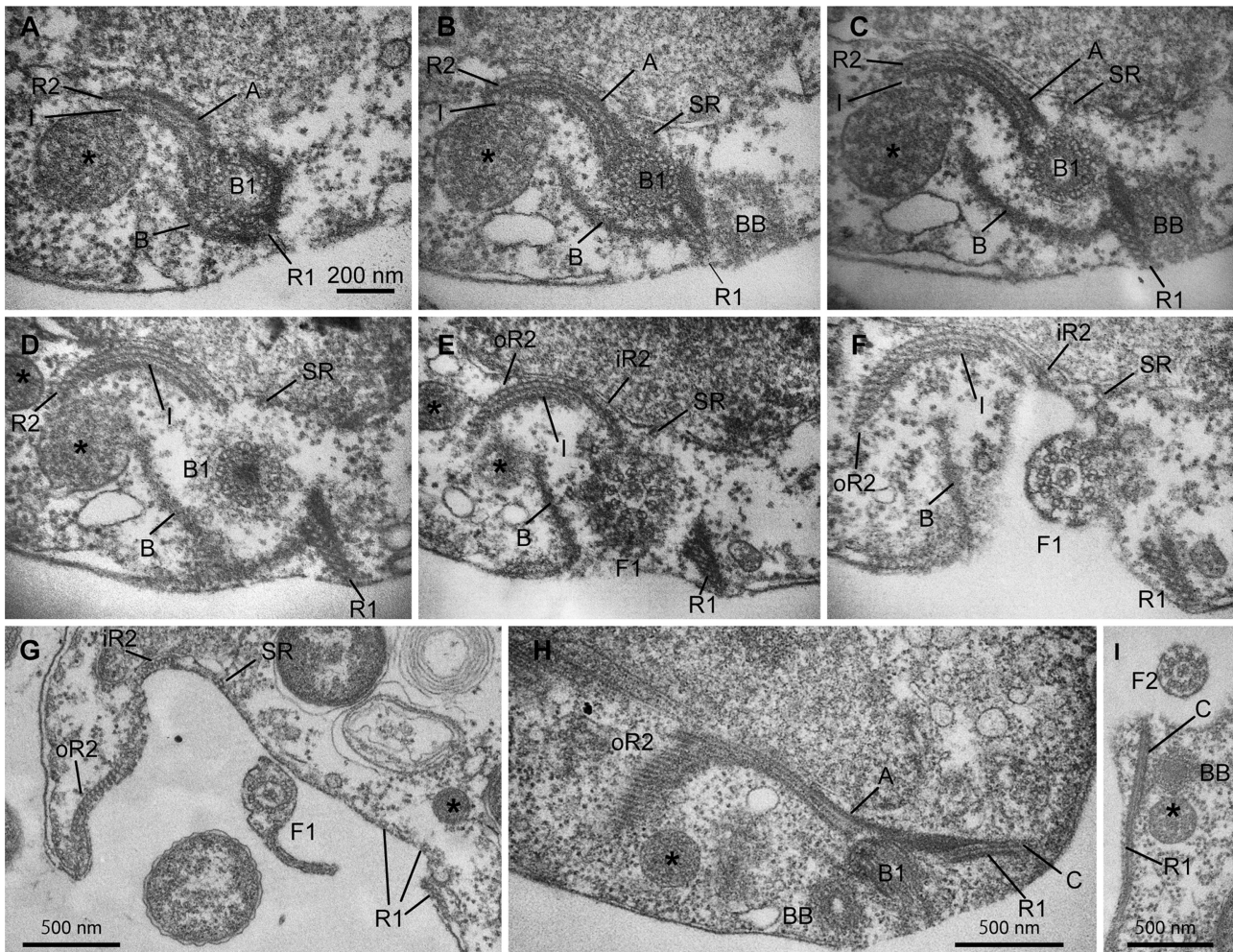


Figure 5. Transmission electron micrographs of *Aduncisulcus paluster* gen. et sp. nov. (NY0171) showing the flagellar apparatus associated with posterior basal body 1. A = A fiber; B = B fiber; B1 = basal body 1; C = C fiber; F1 = flagellum 1; F2 = flagellum 2; I = I fiber; iR2 = inner root 2; N = nucleus; oR2 = outer root 2; SR = singlet root. Asterisk indicates a mitochondrion-related organelle (MRO). **A-F.** Non-consecutive serial sections from the anterior (A) to the posterior (F) end of the cell as viewed from the anterior end. **G.** Transverse section through the middle part of the cell as viewed from the anterior end. **H.** Oblique section near the basal bodies. **I.** Sagittal section through the anterior end of the cell.

division, which in turn contributed to inferences about the earliest stages in the evolution of eukaryotes as a whole (Yubuki et al. 2013; Yubuki and Leander 2013). Previous molecular phylogenetic analyses of fornicates demonstrated that (1) CLOs (and retortamonads) are paraphyletic and (2) *Dysnectes* and *Kipferlia* are more closely related to diplomonads (and *Retortamonas*) than to *Chilomastix* (Fig. 11). The overall diversity of fornicates remains to be determined through exploration of different habitats using several different approaches, including environmental DNA sequence surveys, cultivation experiments and detailed ultrastructural studies. Nonetheless, current molecular phyloge-

netic data combined with the ultrastructural and behavior traits described here enabled us to establish a new genus and species for isolate NY0171.

Taxonomic Summary

Assignment: Eukaryota; Excavata; Metamonada; Fornicata

Aduncisulcus gen. nov. Yubuki and Leander

Description: Free-living, colorless and heterotrophic cells with two heterodynamic flagella.

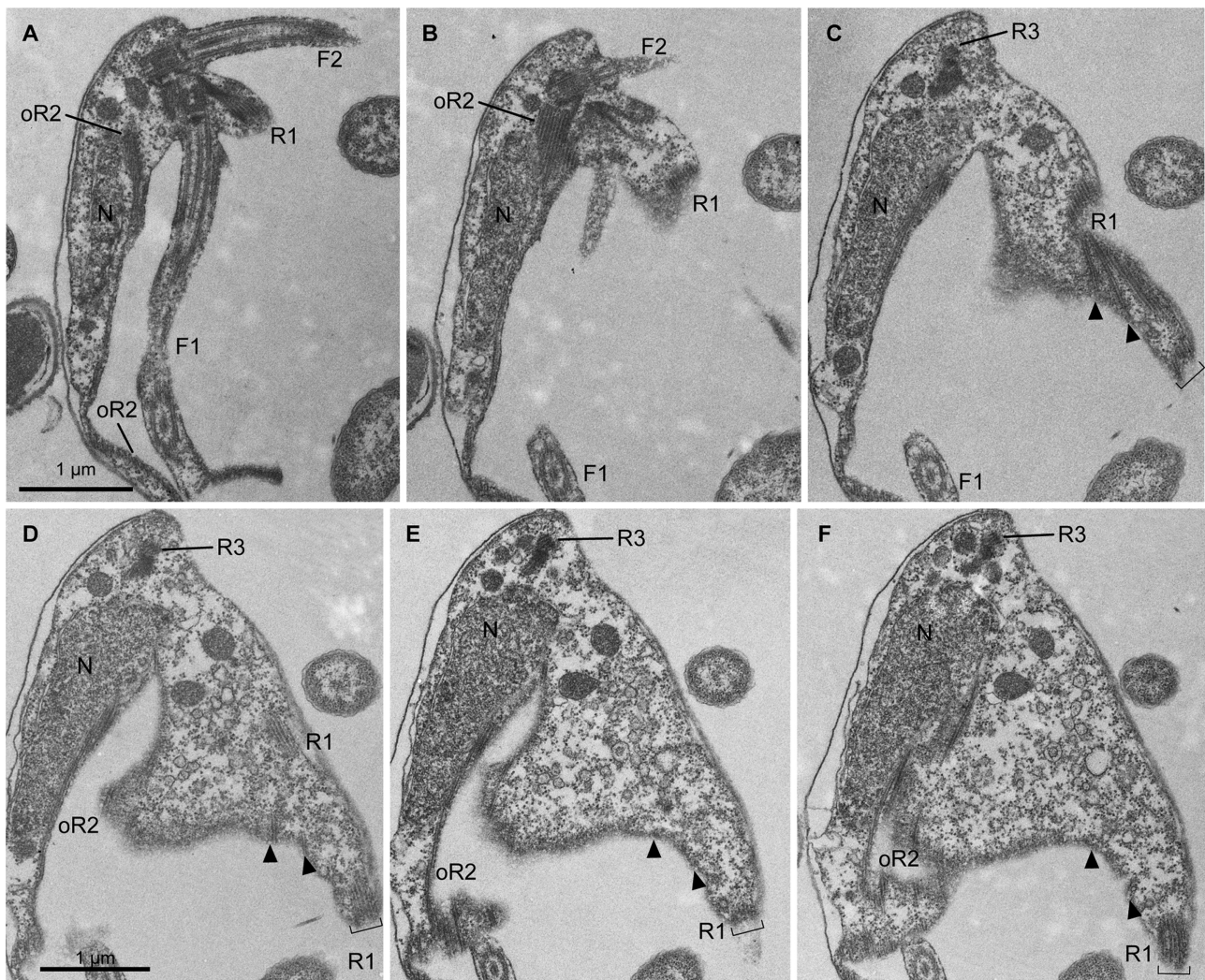


Figure 6. Transmission electron micrographs of *Aduncisulcus paluster* gen. et sp. nov. (NY0171) showing the microtubular roots that support the ventral groove. Consecutive serial sections in a coronal plane from the periphery (A) to the interior (F) of the cell. A=A fiber; F1=flagellum 1; F2=flagellum 2; N=nucleus; oR2=outer root 2; R1=root 1; R3=root 3; SR=singlet root. Arrowheads and asterisk indicate disassociated R1 microtubules and mitochondrion-related organelles (MRO), respectively.

Curved ventral groove with conspicuous cytopharynx at the posterior end. A long ventral vane and a diminutive dorsal vane on the posterior flagellum, F1. F2 inserts laterally. B fiber attaches to the anterior end of R1. Four basal bodies in the flagellar apparatus. Thin C fiber on R1.

Type species: *Aduncisulcus paluster* sp. nov.

Etymology: Latin adjective *aduncus* and noun *sulcus* meaning “hooked” and “groove” in English, respectively, and *-i-* is a Latin connective. The genus name refers to the curved shape of the ventral groove. Gender masculine.

Aduncisulcus paluster sp. nov. Yubuki and Leander

Description: Bean-shaped cells are 8.9 μm (7.0–11.3 μm, n=30,) long and 5.4 μm (4.1–7.2 μm, n=30) wide. Cells attach to substrates using the tip of the posterior flagellum, F1. Cells swim with a constant rotation. Cells possess cytopharynx and robust R3.

Hapantotype: TEM block of *Aduncisulcus paluster* (NY0171), deposited in the collection at Beaty Biodiversity Museum, University of

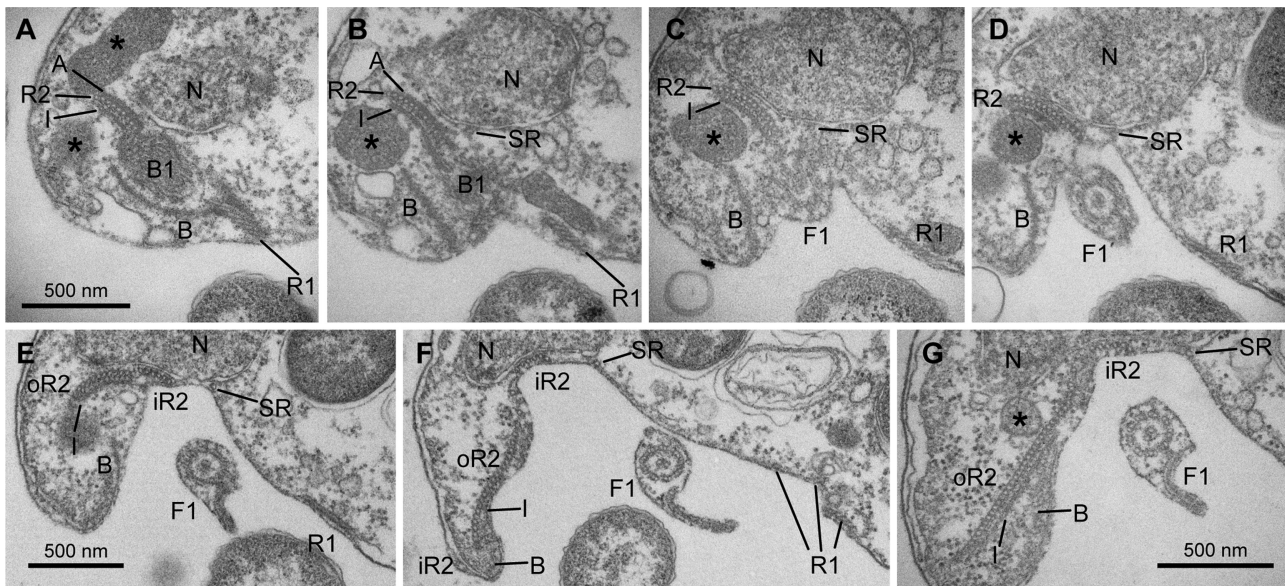


Figure 7. Transmission electron micrographs of *Aduncisulcus paluster* gen. et sp. nov. (NY0171) showing microtubular root 2 (R2) and the singlet root (SR). A = A fiber; B = B fiber; B1 = basal body 1; F1 = flagellum 1; I = I fiber; iR2 = inner root 2; N = nucleus; oR2 = outer root 2; SR = singlet root. Asterisk indicates a mitochondrion-related organelles (MRO). **A-D** and **E-F** are different consecutive serial sections in the transverse plane.

British Columbia, Canada (Accession number: MI-PR128).

Type locality: Ishigaki Island, Okinawa, Japan (24°48'N, 124°23'E)

Type habitat: Low oxygen mangrove sediments.

Type isolate: NY0171

Etymology: The Latin adjective *paluster* means “swampy” or “marshy” in English. The specific epithet refers the habitat where this species was found. The specific epithet agrees with the masculine gender of the generic name *Aduncisulcus*.

DNA sequence: A nearly complete sequence of the small subunit (SSU) rRNA gene of the type isolate, NY0171, was reported by [Kolisko et al. \(2010\)](#) and has the Genbank accession number, GU827603.

Methods

The culture strain *Aduncisulcus paluster* gen. et sp. nov. (NY0171): The strain of *A. paluster* examined here was the same strain studied by [Takishita et al. \(2012\)](#) and [Kolisko et al. \(2010\)](#) as “CL2”. The culture was derived from a mangrove sediment sample collected from Ishigaki Island, Okinawa, Japan (24°48'N, 124°23'E) on September 19th, 2005. The cell cultures were maintained at 16 °C in seawater with modified TYGM-9 medium (final concentration 10%) under low oxygen concentration. Preparation of the modified TYGM-9 medium

was described in [Yubuki et al. \(2013\)](#). The type culture, NY0171, is available upon request.

Light microscopy: Live cells were observed with a Zeiss Axioplan 2 microscope equipped with a Leica DC500 digital camera.

Scanning electron microscopy: Cells were washed with anoxic seawater several times before being mixed with an equal volume of fixative containing 2.5% (v/v) glutaraldehyde and 0.2 M sucrose in 0.2 M sodium cacodylate buffer (SCB) (pH 7.2). The specimen was mounted on glass plates coated with poly-L-lysine for 1.5 h on ice. The glass plates were rinsed with 0.2 M SCB containing 0.2 M sucrose and fixed in 1% osmium tetroxide for 1 h. The fixed cells were then rinsed with 0.2 M SCB and dehydrated with a graded ethanol series from 30% to absolute ethanol. Samples were critical point dried with CO₂ using a Tousimis critical point dryer. Samples were then coated with gold using a Cressington 208HR high-resolution sputter coater, and observed with a Hitachi S-4700 field emission scanning electron microscope.

Transmission electron microscopy: For ultra-thin sections, cells were washed with anoxic seawater several times before being suspended in a mixture of 5% glutaraldehyde and 0.2 M sucrose in 0.2 M SCB (pH 7.2) at room temperature for one hour. Cells were concentrated into a pellet by centrifugation at 1000 g for 10 min, then rinsed with 0.2 M SCB (pH 7.2). The suspension was then fixed in 1% osmium tetroxide in 0.2 M SCB (pH 7.2) at room temperature for one hour, followed by dehydration through an ethanol series and substitution with acetone. The cells were infiltrated with an acetone-resin (Epon 812) mixture and ultimately embedded in absolute resin. Serial ultra-thin sections were cut on a Leica EM UC6 ultramicrotome with a diamond knife and double stained with 2% (w/v) uranyl acetate and lead citrate ([Reynolds 1963](#)). The ultra-thin sections were observed using a Hitachi H7600 electron microscope.

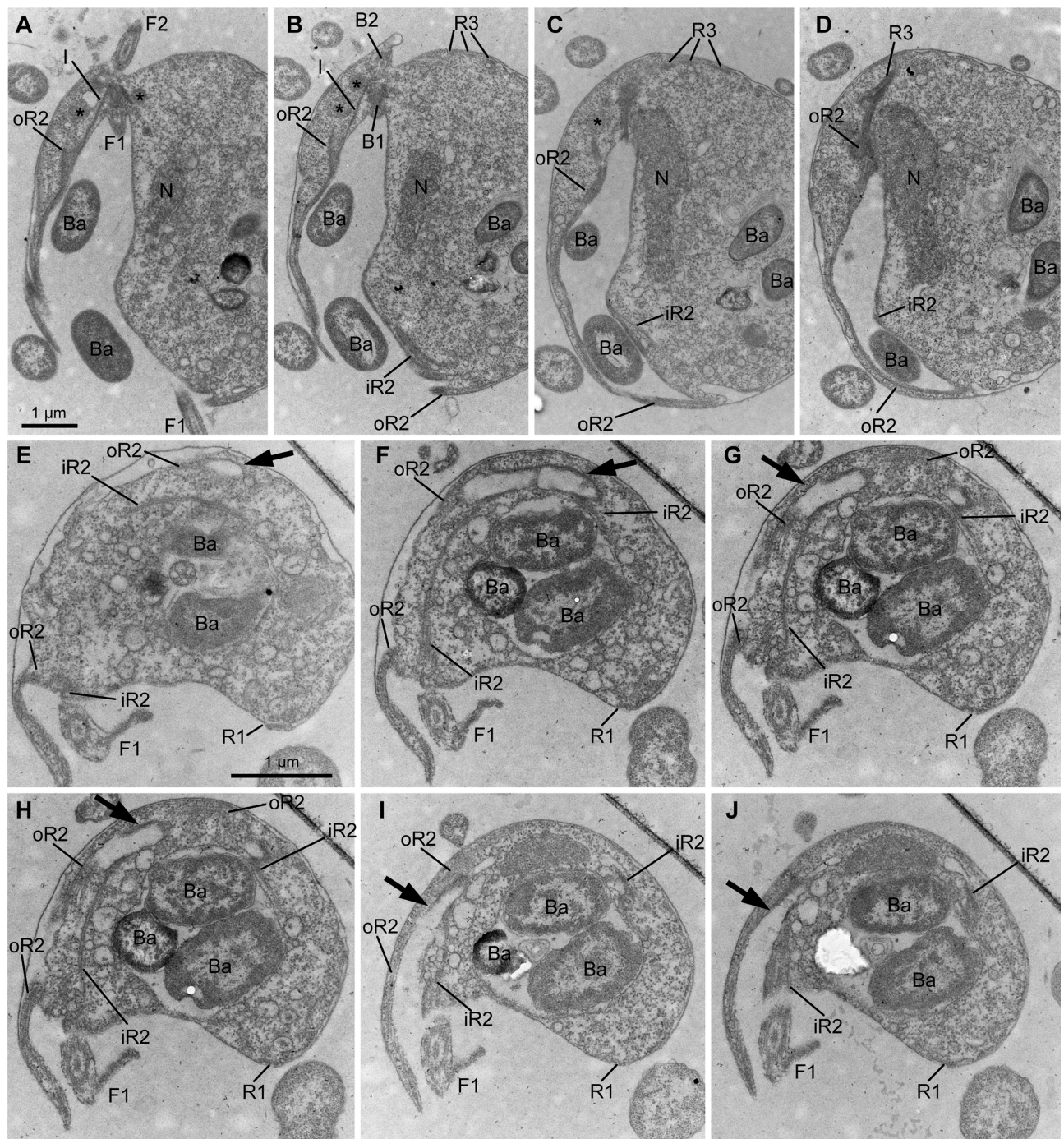


Figure 8. Transmission electron micrographs of *Aduncisulcus paluster* gen. et sp. nov. (NY0171) showing the cytopharynx (arrow) and the supporting roots at the posterior end of the cell. **A-D.** Non-consecutive serial sections through the coronal plane. **E-J.** Non-consecutive serial sections through the transverse plane. B = B fiber; Ba = bacterium; B1 = basal body 1; B2 = basal body 2; F1 = flagellum 1; F2 = flagellum 2; I = I fiber; iR2 = inner root 2; N = nucleus; oR2 = outer root 2; R1 = root 1; R3 = root 3. Asterisk indicates a mitochondrion-related organelle (MRO).

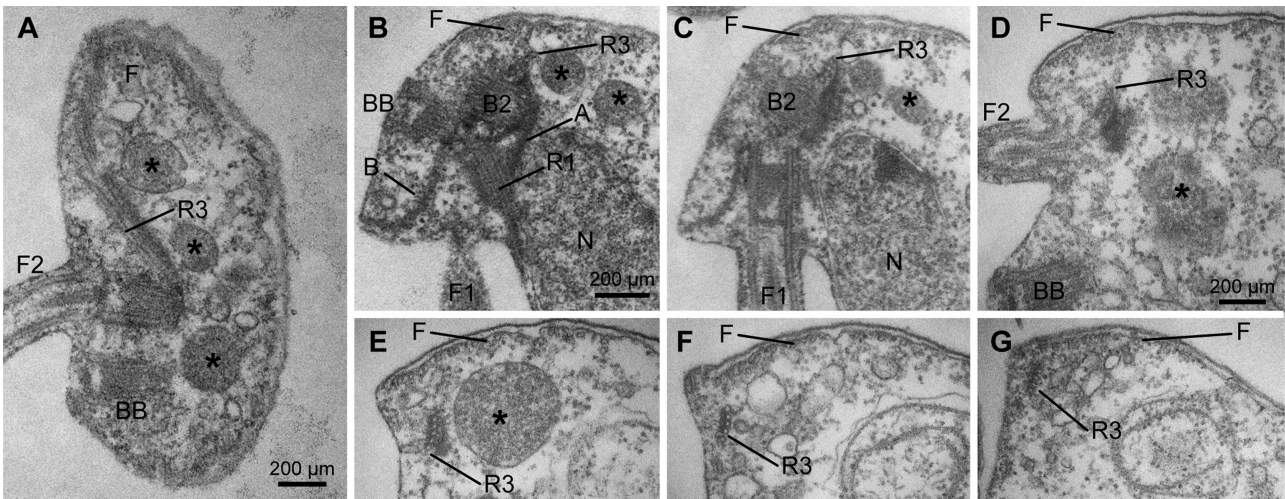


Figure 9. Transmission electron micrographs of *Aduncisulcus paluster* gen. et sp. nov. (NY0171) showing microtubular root 3 (R3). **B-C** and **D-G** are two different sets of non-consecutive serial sections through the anterior part of the cell. A=A fiber; B=B fiber; BB=barren basal body; B2=basal body 2; F=dorsal fan; F1=flagellum 1; F2=flagellum 2; N=nucleus; R1=root 1; R3=root 3. Asterisk indicates a mitochondrion-related organelles (MRO).

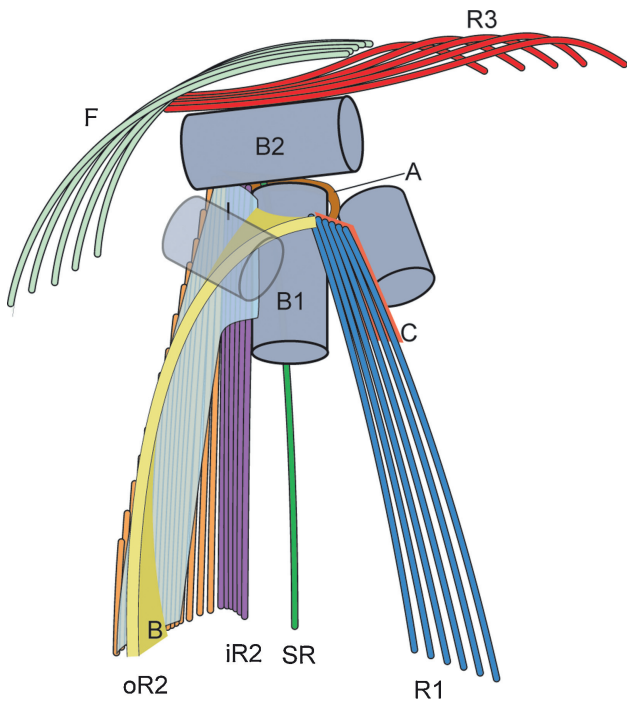


Figure 10. An illustration of the flagellar apparatus of *Aduncisulcus paluster* gen. et sp. nov. (NY0171) as viewed from ventral side of the cell. A=A fiber; B=B fiber; C=C fiber; B1=basal body 1; B2=basal body 2; F=dorsal fan; I=I fiber; R1=root 1; iR2=inner root 2; oR2=outer root 2; R3=root 3; SR=single root.

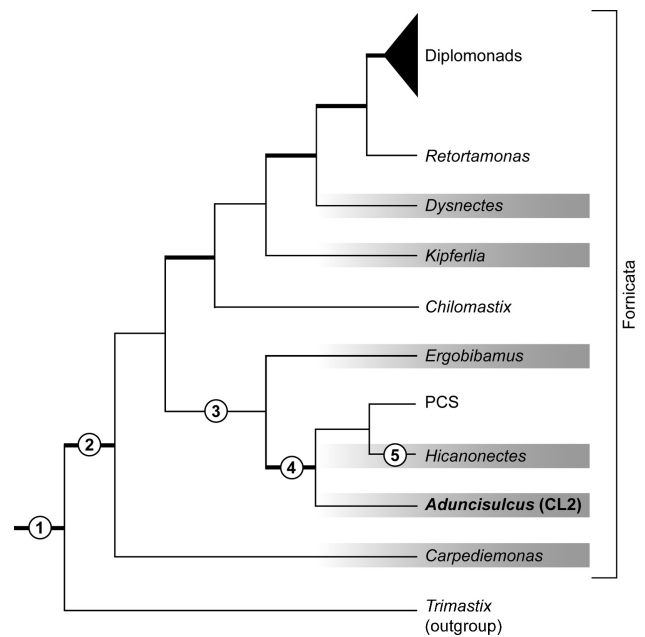


Figure 11. A phylogenetic tree showing position of *Aduncisulcus paluster* gen. et sp. nov. (NY0171) within the Fornicata. The branching pattern reflects a phylogenetic tree inferred from a multi-gene dataset; thick branches indicate robust statistical support in the analyses (Takishita et al. 2012). Shaded lineages are CLOs. See the text for the trait changes indicated by numbers. Additional inferences about trait changes within the Fornicata are described in Yubuki et al. (2013).

Acknowledgements

This work was supported by the Tula Foundation's Center for Microbial Diversity and Evolution at the University of British Columbia. BSL was also supported by the Canadian Institute for Advanced Research, Program in Integrated Microbial Biodiversity.

References

- Adl SM, Simpson AGB, Lane CE, Lukeš J, Bass D, Bowser SS, Brown MW, Burki F, Dunthorn M, Hampl V, Heiss AA, Hoppenrath M, Lara E, le Gall L, Lynn DH, McManus H, Mitchell EAD, Mozley-Stanridge SE, Parfrey LW, Pawlowski J, Rueckert S, Shadwick L, Schoch CL, Smirnov A, Spiegel FW** (2012) The revised classification of eukaryotes. *J Eukaryot Microbiol* **59**:429–514
- Bernard C, Simpson AGB, Patterson DJ** (1997) An ultrastructural study of a free-living retortamonad, *Chilomastix cuspidata* (Larsen & Patterson, 1990) n. comb. (Retortamonadida, Protista). *Europ J Protistol* **33**:254–265
- Brugerolle G** (1977) Ultrastructure du genre *Retortamonas* Grassi 1879 (Zoomastigophorea: Retortamonadida Wenrich 1931). *Protistologica* **13**:233–240
- Brugerolle G, Lee JJ** (2000) Oder Diplomonadida. In Lee JJ, Leedale GF, Bradbury P (eds) *The Illustrated Guide to the Protozoa*. Soc. Protozool., Lawrence, KS, pp 1125–1135
- Cavalier-Smith T** (1998) A revised six-kingdom system of life. *Biol Rev Camb Philos Soc* **73**:203–266
- Kolisko M, Silberman JD, Cepicka I, et al.** (2010) A wide diversity of previously undetected free-living relatives of diplomonads isolated from marine/saline habitats. *Environ Microbiol* **12**:2700–2710
- Moestrup Ø** (2000) The Flagellate Cytoskeleton: Introduction of a General Terminology for Microtubular Flagellar Roots in Protists. In Leadbeater BSC, Green JC (eds) *The Flagellates. Unity, Diversity, Evolution*. Taylor & Francis, London, pp 69–94
- O'Kelly CJ, Farmer MA, Nerad TA** (1999) Ultrastructure of *Trimastix pyriformis* (Klebs) Bernard et al: similarities of *Trimastix* species with retortamonad, jakobid flagellates. *Protist* **150**:149–162
- Park JS, Kolisko M, Simpson AGB** (2010) Cell morphology, formal description of *Ergobibamus cyprinoides* n. g., n. sp., another *Carpediemonas*-like relative of diplomonads. *J Eukaryot Microbiol* **57**:520–528
- Park JS, Kolisko M, Heiss AA, Simpson AGB** (2009) Light microscopic observations, ultrastructure, molecular phylogeny of *Hicanonectes teleskopos* n. g., n. sp., a deep-branching relative of diplomonads. *J Eukaryot Microbiol* **56**:373–384
- Reynolds ES** (1963) The use of lead citrate at high pH as an electron-opaque stain in electron microscopy. *J Cell Biol* **17**:208–212
- Silberman JD, Simpson AGB, Kulda J, Cepicka I, Hampl V, Johnson PJ, Roger AJ** (2002) Retortamonad flagellates are closely related to diplomonads—implications for the history of mitochondrial function in eukaryote evolution. *Mol Biol Evol* **19**:777–786
- Simpson AGB** (2003) Cytoskeletal organization, phylogenetic affinities, systematics in the contentious taxon Excavata (Eukaryota). *Int J Syst Evol Microbiol* **53**:1759–1777
- Simpson AGB, Patterson DJ** (1999) The ultrastructure of *Carpediemonas membranifera* (Eukaryota) with reference to the “Excavate hypothesis”. *Eur J Protistol* **35**:353–370
- Simpson AGB, Roger AJ** (2004) Excavata, the Origin of Amitochondriate Eukaryotes. In Hirt RP, Horner DS (eds) *Organelles, Genomes, Eukaryote Phylogeny – an Evolutionary Synthesis in the Age of Genomics*. CRC Press, Boca Raton, FL, pp 27–53
- Simpson AGB, Bernard C, Patterson DJ** (2000) The ultrastructure of *Trimastix marina* Kent, 1880 (Eukaryota), an excavate flagellate. *Europ J Protistol* **36**:229–251
- Simpson AGB, Inagaki Y, Roger AJ** (2006) Comprehensive multigene phylogenies of excavate protists reveal the evolutionary positions of “primitive” eukaryotes. *Mol Biol Evol* **23**:615–625
- Stairs CW, Leger MM, Roger AJ** (2015) Diversity and origins of anaerobic metabolism in mitochondria and related organelles. *Phil Trans R Soc B* **370**:20140326
- Takishita K, Kolisko M, Komatsuzaki H, Yubuki A, Inagaki Y, Cepicka I, Smejkalová P, Silberman JD, Hashimoto T, Roger AJ, Simpson AGB** (2012) Multigene phylogenies of diverse *Carpediemonas*-like organisms identify the closest relatives of “amitochondriate” diplomonads, retortamonads. *Protist* **163**:344–355
- Yubuki N, Leander BS** (2013) Evolution of microtubule organizing centers across the tree of eukaryotes. *Plant J* **75**:230–244
- Yubuki N, Simpson AGB, Leander BS** (2013) Comprehensive ultrastructure of *Kipferlia bialata* provides evidence for character evolution within the Fornicata (Excavata). *Protist* **164**:423–439
- Yubuki N, Čepička I, Leander BS** (2016) Evolution of the microtubular cytoskeleton (flagellar apparatus) in parasitic protists. *Mol Biochem Parasitol* (in press)
- Yubuki N, Inagaki Y, Nakayama T, Inouye I** (2007) Ultrastructure, ribosomal RNA phylogeny of the free-living heterotrophic flagellate *Dysnectes brevis* n. gen., n. sp., a new member of the Fornicata. *J Eukaryot Microbiol* **54**:191–200

Available online at www.sciencedirect.com

ScienceDirect